ASEG-PESA 2015
Geophysics and Geology together for Discovery
24th International Geophysical Conference and Exhibition
15 – 18 February 2015 Perth, Western Australia

The 3D joint inversion of MT and ZTEM data

Daniel Sattel
EM Solutions LLC
Golden, CO, USA
dsattel@comcast.net

Ken Witherly
Condor Consulting, Inc.
Lakewood, CO, USA
ken@condorconsult.com

SUMMARY

MT and ZTEM data were inverted with a number of 2D and 3D algorithms to recover the subsurface conductivity structure of an area of interest. A 2D inversion algorithm was used to model the magnetotelluric TM and TE mode impedances and the ZTEM tipper data, separately. The derived conductivity-depth sections don't show much agreement, possibly indicating the conductivity structure of the area to be highly three-dimensional.

A 3D inversion algorithm was used to invert the MT and ZTEM data, separately and jointly. Overall, there is good agreement between the derived conductivity structures. This suggests that a joint inversion can extract successfully the combined subsurface conductivity information from the two data sets.

Key words: 2D inversion, 3D inversion, AFMAG, MT, ZTEM.

INTRODUCTION

The ZTEM system developed and operated by Geotech Ltd (Legault, 2012) is an AFMAG system that measures the vertical magnetic field from the air, while recording the horizontal magnetic-field components at a base station. AFMAG is related to the better-known magnetotelluric (MT) method. However, whereas AFMAG surveys acquire only magnetic field data, MT surveys measure the electric and magnetic fields along a traverse or on a grid. As a result, the derived ZTEM tipper data are only sensitive to lateral conductivity contrasts, whereas the derived MT impedance data are sensitive to the actual values of the subsurface conductivities. When jointly inverted, the data from both methods complement each other, with the airborne ZTEM data providing good spatial coverage and the MT data providing the resolution of the background conductivity structure (Wannamaker and Legault, 2014; Hübert et al., 2013).

For the modelling of MT and ZTEM data, plane wave excitation is assumed, and algorithms developed originally for the 2D and 3D modelling of MT data (Farquharson et al., 2002; Wannamaker et al., 1987; Sasaki, 2001) have since been modified to allow for the modelling of ZTEM data (Legault et al., 2012; Sattel and Witherly, 2012; Holtham and Oldenburg, 2010a; Sasaki et al., 2013). Some of these algorithms now allow for the joint inversion of MT and ZTEM data (Wannamaker and Legault, 2014; Holtham and Oldenburg, 2010b).

For this study, we have used modified versions of a 2D MT inversion algorithm developed by Constable and Wannamaker (deGroot-Hedlin and Constable, 1990; Wannamaker at al., 1987; deLugao and Wannamaker, 1996) and the 3D MT/ZTEM inversion algorithm discussed by Holtham and Oldenburg (2010a, 2010b).

After comparing synthetic MT and ZTEM data derived with 2D and 3D modelling algorithms as a consistency check, we discuss 2D and 3D inversion results obtained from inverting MT and ZTEM survey data separately and jointly.

SYNTHETIC DATA

The MT impedances and ZTEM responses across a 10 S conductor in a 1000 Ohm-m half-space derived by the 2D and 3D algorithms are shown in Figure 1. A strike length of 10 km was modelled for the 3D model. For the TE-mode data, the agreement between 2D and 3D results is excellent. For the TM-mode and ZTEM data the agreement is also very good. These results confirm that a suitable set of model parameters was selected, and that consistent results are obtained from these algorithms.

FIELD DATA

The MT and ZTEM survey data were recently acquired across an area of interest. The location of the MT stations and the ZTEM flight lines are shown in Figure 2. A fixed remote reference MT station (30 km to south-southwest) was maintained, which allowed for the processing of recorded time series using robust remote referencing techniques (Chave and Thomson, 2004). The acquisition of MT data by Western Geco in the frequency range 0.1-10,000 Hz did not include the recording of vertical magnetic field data. Hence, MT tipper data were unavailable for this data set.

Preliminary results indicated little differences between inverting impedance data and apparent resistivity / phase data. All of the MT inversion results discussed in the following were derived from the impedance data. The impedance skews (Swift, 1967) are shown in Figure 3 as a function of frequency and as a grid at 252 Hz. With many values exceeding 0.5 the skews indicate a three-dimensional conductivity structure almost everywhere in the survey area.

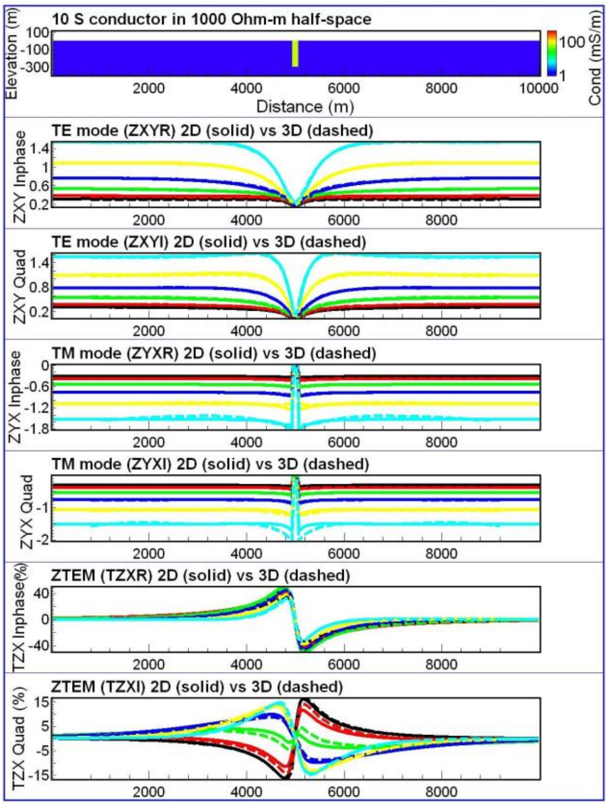

Figure 1. Synthetic 2D (solid) and 3D (dashed) responses across 10 S conductor in a 1,000 Ohm-m half-space model. MT TE-mode impedances (top), MT TM-mode impedances (centre) and ZTEM tipper data (bottom).

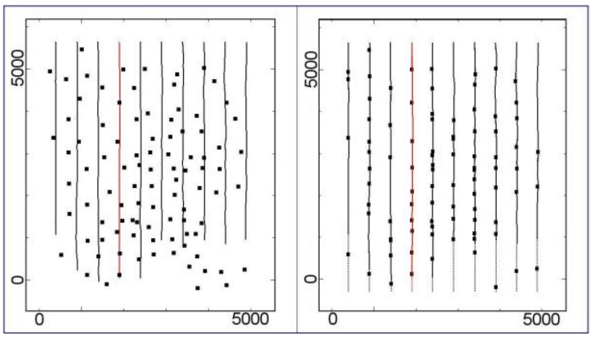

Figure 2. Location of MT stations (dots) and ZTEM flight lines (left); MT stations (dots) projected on extended ZTEM flight lines (right), indicating 3D model block. The traverse shown in Figures 4-8 is shown in red.

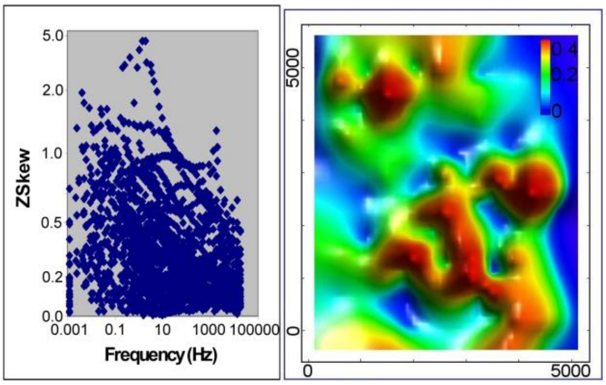

Figure 3. Distribution of derived impedance skews (left) and grid of impedance skew at 252 Hz (right).

2D Inversions

Synthetic MT traverses for 2D inversion were generated from the field data by projecting the station locations onto the ZTEM flight lines. This also allowed for a direct comparison between conductivity-depth sections derived by 2D inversion from MT and ZTEM data. MT data in the frequency range 0.001 – 17,640 Hz were included in the 2D inversion. Model cells are 20 m wide and 25 m thick at the surface, increasing in size with depth. The result of the TE-mode and TM-mode data inversions along one of the synthetic traverses is shown in Figures 4-5. The corresponding ZTEM data (30-360 Hz) results are shown in Figure 6. The 2D inversions fit the data very well. However, it is hard to find much agreement between the conductivity-depth sections derived from the MT TE-mode, TM-mode and ZTEM data. As already indicated by the impedance skew data, the conductivity structure might just be too complex to be recoverable reliably by a 2D inversion.

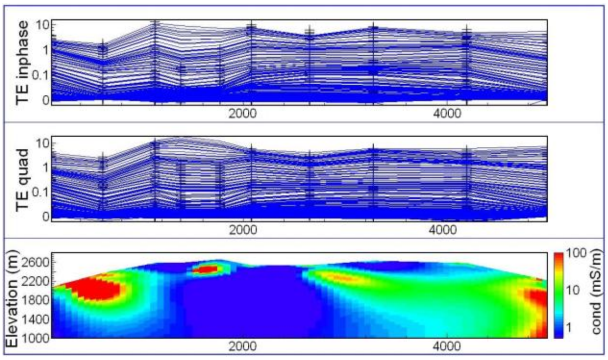

Figure 4. Observed (black crosses) and modelled (blue lines) MT TE-mode data with 2D-inverted conductivity-depth section (CDS).

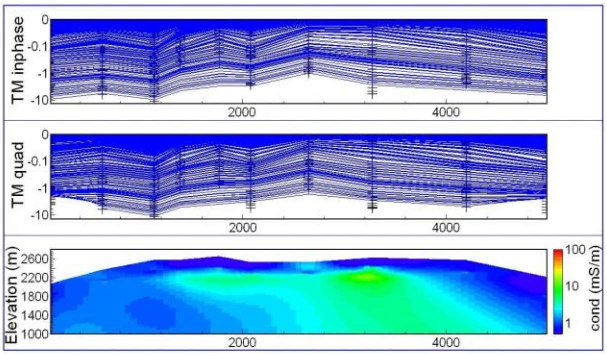

Figure 5. Observed (black crosses) and modelled (blue lines) MT TM-mode data with 2D-inverted CDS.

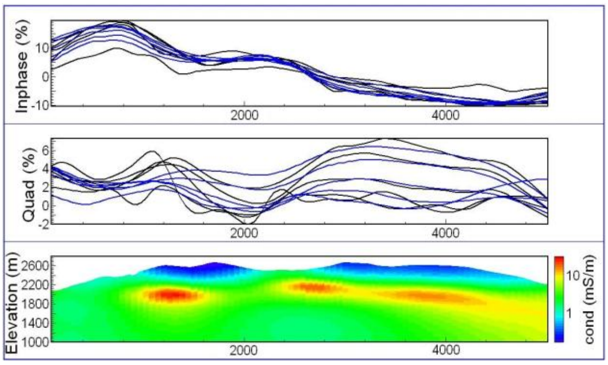

Figure 6. Observed (black) and modelled (blue) ZTEM data with 2D-inverted CDS.

3D Inversions

Data modelled by the 3D inversion include the MT data in the frequency range 1 – 680 Hz and the ZTEM data (30-360 Hz). These data sets were inverted separately and jointly. Model cells are 100x100 m wide and 25 m thick at the surface, increasing in size with depth. For comparison with the 2D model results, conductivity-depth sections and data profiles were extracted along the same traverse as shown in Figures 4-6. These results are shown in Figures 7-9, and conductivity grids are shown in Figure 10. The results of the separate inversions show a fairly good data fit and their conductivity models are quite similar. The sections show some model discrepancies at the southern end, where, unlike the MT model, the ZTEM sections indicate a conductor beneath the surface resistor. A comparison of the conductivity grids shows the joint inversion result to combine features of the two other grids.

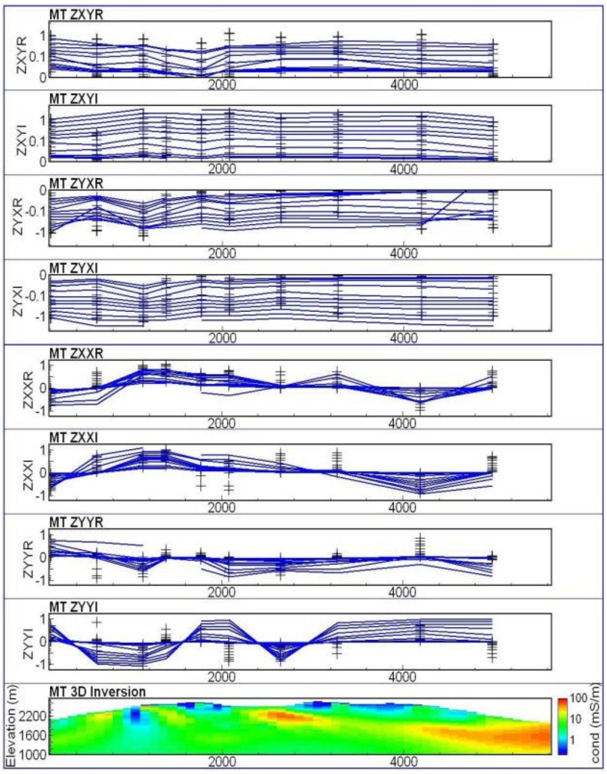

Figure 7. 3D MT data inversion. Observed (black crosses) and modelled (blue lines) MT data with derived conductivity-depth section (CDS).

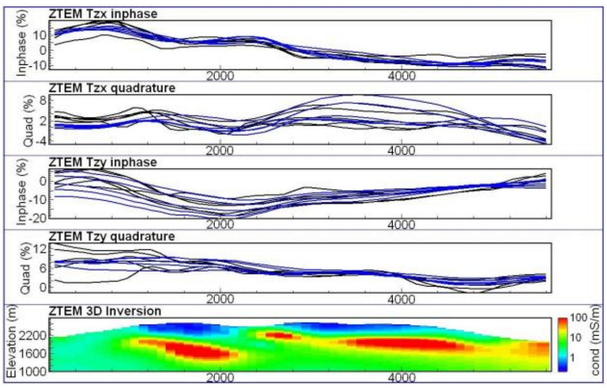

Figure 8. 3D ZTEM inversion. Observed (black) and modelled (blue) ZTEM data with derived CDS.

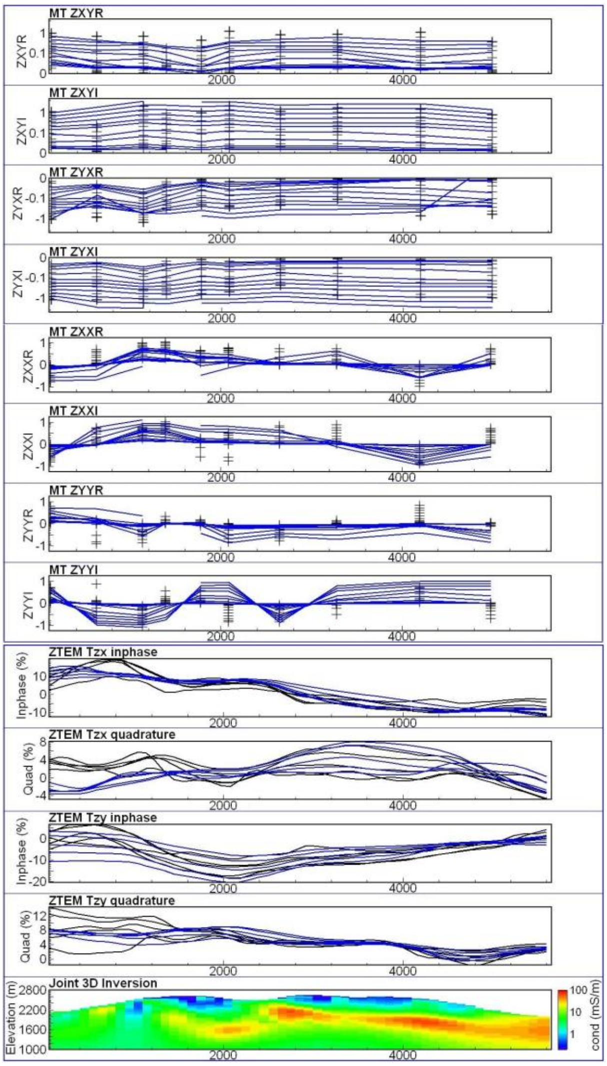

Figure 9. 3D joint MT – ZTEM inversion. Observed (black) and modelled (blue) MT and ZTEM data with derived CDS.

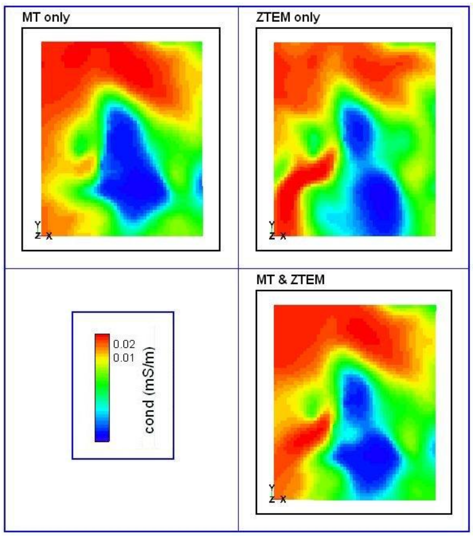

Figure 10. Conductivity-depth slices at Z=1450 m derived from 3D inversion of the MT data (top left) and ZTEM data (top right), and from the MT and ZTEM data jointly (bottom).

A comparison of selected observed and modelled MT and ZTEM responses is shown in grid form in Figure 11. For ZTEM, total phase-rotated (TPR) inphase grids are shown. TPR grids are produced by adding phase-rotated Tzx and Tzy grids together and present the data in a form that is useful for quick data assessment (Sattel and Witherly, 2012). The comparison of the TPR grids shows that most of the structures indicated on the observed data grid have been mapped by the 3D joint inversion. The grids of Figure 11 also show that the stand-alone inversions provide an acceptable fit to the MT data and a very good fit to the ZTEM data. Further, there is little difference between the modelled responses of the stand-alone inversions and the joint inversion, i.e. the joint inversion was able to derive a conductivity model that was agreeable with both data sets.

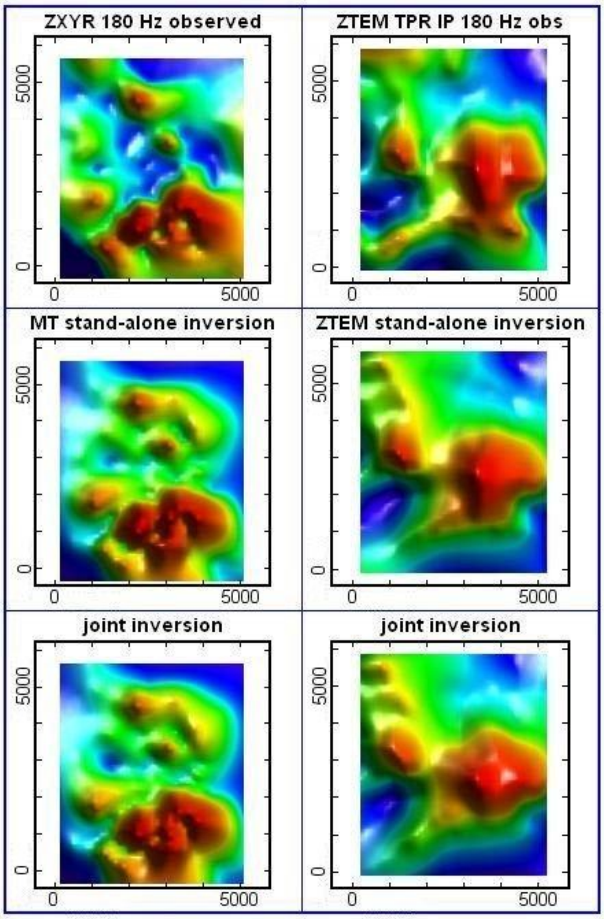

Figure 11. MT (ZXYR 180 Hz, left) and ZTEM (TPR IP 180 Hz, right) responses of observed data (top), responses modelled by MT and ZTEM stand-alone inversions (centre) and responses modelled by joint inversion (bottom).

CONCLUSIONS

MT and ZTEM data were modelled with 2D and 3D inversions. The results indicate that for the investigated MT and ZTEM data, 2D inversions are inadequate to derive the subsurface conductivity structure. The 3D inversion results derived from the various data sets are fairly consistent, which indicates that the joint 3D inversion of MT and ZTEM data can successfully extract the subsurface conductivity structure from a combination of these data.

REFERENCES

Chave, A.D., and Thomson, D.J., 2004, Bounded influence magnetotelluric response function estimation, Geophysical Journal International, **157**, 988-1006.

DeGroot-Hedlin, C. and S. Constable, 1990, Occam's inversion to generate smooth two-dimensional models from magnetotelluric data: Geophysics 55, 1613-1624.

De Lugao, P.P., and Wannamaker, P., 1996, Calculating the two-dimensional magnetotelluric Jacobian in finite elements using reciprocity, Geophys. J. Int., 127, 806-810.

Farquharson, C.G., Oldenburg, D.W, Haber, E., and Shekhtman, R., 2002, An algorithm for the three-dimensional inversion of magnetotelluric data: *72nd International Exposition and Annual Meeting, SEG, Expanded Abstracts*, 649-652.

Holtham, E., and Oldenburg, D.W., 2010a, Three-dimensional inversion of ZTEM data: Geophys. J. Int. 182, 168-182.

Holtham, E., and Oldenburg, D.W., 2010b, Three-dimensional inversion of MT and ZTEM data: *80th International Exposition and Annual Meeting, SEG, Expanded Abstracts*.

Hübert, J., Lee, B., Unsworth, M., Richards, J., Oldenburg, D., Cheng, L.Z., 2013, Imaging a Ag-Au rich epithermal system in British Columbia, Canada with airborne ZTEM and ground Magnetotelluric data: *83rd International Exposition and Annual Meeting, SEG, Expanded Abstracts*.

Legault, J.M., 2012, Ten years of passive airborne AFMAG EM development for mineral exploration: *82nd International Exposition and Annual Meeting, SEG, Expanded Abstracts*.

Legault, J., Wilson, G.A., Gribenko, A.V., Zhdanov, M.S., Zhao, S., and Fisk, K., 2012, An overview of the ZTEM and AirMt airborne EM systems: a case study from the Nebo-Babel Ni-Cu-PGE deposit, West Musgrave, W.A.: *Preview*, **158**, 26-32.

Sasaki, Y., 2001, Full 3D inversion of electromagnetic data on PC: Journal of Applied Geophysics, **46**, 45-54.

Sasaki, Y., Yi, M.-J., and Choi, J., 2013, 3D inversion of ZTEM data for uranium exploration: *23rd International Geophysical Conference and Exhibition, ASEG-PESA, Extended Abstracts.*

Sattel, D., and Witherly, K., 2012, An overview of ZTEM interpretation tools, In R.J.L. Lane (editor), *Natural Fields EM Forum 2012: Abstracts from the ASEG Natural Fields EM Forum 2012: Published by Geoscience Australia, Geoscience Australia Record 2012/04*.

Swift, C.M., Jr, 1967, A magnetotelluric investigation of an electrical conductivity anomaly in the southwestern United States: PhD thesis, MIT.

Wannamaker, P.E., Stodt, J.A., and Rijo, L., 1987, A stable finite-element solution for two-dimensional magnetotelluric modeling: *Geophysical Journal of the Royal Astronomical Society*, **88**, 277-296.

Wannamaker, P.E., and Legault, J.M., 2014, Two-dimensional joint inversion of MT and ZTEM data plane-wave EM data: *GeoConvention 2014, Expanded Abstracts.*